JOURNAL OF RENEWABLE AND SUSTAINABLE ENERGY **10**, 023703 (2018)

Modeling, simulation, and optimization of a solar water heating system in different climate regions

Kaan Yaman and Gökhan Arslan[a)]

Department of Mechanical Engineering, Mersin University, 33343 Mersin, Turkey

(Received 11 September 2017; accepted 20 February 2018; published online 9 March 2018)

To design an effective solar water heating system (SWHS), parameters such as the energy consumption rate, total cost, and climatic region characteristics must be analyzed during the time interval (annual or seasonal) of the predicted use. In this paper, the optimum dimensions of a SWHS were determined using the life cycle cost (LCC) analysis constraint by the 40% solar fraction for the different regions of Turkey for annual and seasonal periods. Particle swarm optimization/Hooke and Jeeves hybrid optimization algorithm was applied. The optimum number of solar collectors and the volume of the hot water storage tank of the SWHS were determined. The optimization process showed that LCC could be reduced for all regions in the range of 3.3%–5.8% in the annual simulation period and 1.8%–4.8% in the period of the summer season simulation. The optimization process carried out in the winter season revealed that the optimization results obtained over different time periods can make a difference in the relations between the optimization parameters. Accordingly, the performance of the SWHS could be improved using a design according to the optimum results obtained at the time interval of the usage. The optimization results obtained in the summer season led to a saving in LCC, while the results obtained in the winter season led to an improvement in the system's thermal performance. Finally, the relative influence of possible operating parameters on an optimum SWHS was investigated through sensitivity analysis. *Published by AIP Publishing.* https://doi.org/10.1063/1.5004069

I. INTRODUCTION

According to the European Commission - Eurostat solar energy statistics, annual primary production of solar thermal energy is 828 ktoe (34 646 TJ) in 2015 for Turkey and 65% of the produced energy is consumed in the residential sector. In that sector, almost all the solar thermal energy was provided by solar thermal systems that were used for heating domestic hot water (DHW), mainly by small-scale systems in single-family houses and larger applications attached to multi-family houses, hotels, schools, etc.[1] Over the last 10 years, solar thermal energy production has increased by about 2 times, and according to the policy implemented by the Turkish government, it is obvious that this increase will continue in the future. Solar water heating systems (SWHSs) are generally known for high initial cost and low operating cost. These systems need to be carefully evaluated, especially given the increase of solar energy applications in recent years. In this evaluation, the SWHS components must be designed considering the effect of climate, energy, and cost on satisfying the thermal and economic conditions. One of the base issues in solar energy applications is the time discrepancy between solar energy employability and thermal demand. Material savings can be increased, and system performance can be further improved by creating a design that takes into account the seasonal climatic conditions and the variety of the intended use of the systems.

[a)]Author to whom correspondence should be addressed: garslan@mersin.edu.tr

In the literature, SWHS design methods are classified into two categories as correlation-based and simulation-based. Commonly used correlation-based methods include Φ,[2], $\overline{\Phi}$,[3] *f*-chart,[4] and $\overline{\Phi}$, *f*-chart[5] methods. These methods have been successfully implemented by some researchers[6] despite various limitations such as different usage profiles and climatic data. On the other hand, simulation-based methods such as EnergyPlus,[7] Transient System Simulation (TRNSYS),[8] and WATSUN[9] have been implemented along with the development of technology. In particular, after 2006, there has been an increasing trend towards studies concerning the optimization of SWHS (indexed between 1966 and 2017 by SciVerse Scopus of Elsevier). Various researchers numerically and/or experimentally investigated the effect of various design variables on system performance using comprehensive optimization algorithms, such as genetic algorithm (GA), particle swarm optimization (PSO) algorithm, and Hooke and Jeeves (HJ) algorithm (e.g., Refs. 10 and 11). Examples of these studies are as follows: Skerlić *et al.*[12] used the HJ algorithm to find optimum solutions for an SWHS. To obtain the highest solar fraction (SF) (for Belgrade over 3-, 6-, and 12-month periods), the optimum solar collector inclination angle was determined. Using the optimum collector inclination angle in the SWHS, it was shown that the energy consumption can be reduced by 4.7%.[12] Similar to the HJ algorithm, GA has been used in several optimization problems.[11,13] Ko[11] used GA to create optimum configurations and sizing for the capacity and quantity of solar collectors, storage tanks, and auxiliary heaters. Atia *et al.*[13] obtained optimum solutions using GA in which solar energy solely supplied up to 98% for system operation. In their optimization study, Bornatico *et al.*[14] suggested that by using the PSO algorithm instead of GA, investment cost was reduced by 30%, improvement in energy consumption was 3.8%, and the solar fraction was increased by 17.5%. In some studies, hybrid algorithms were used.[15,16] Thus, researchers combine advantages of algorithms to converge the optimization problem in an efficient way. Ng Cheng Hin and Zmeureanu[15] observed that the PSO/HJ hybrid algorithm reduced the life cycle cost (LCC) of the solar combisystem by 19%, the life cycle energy use by 34%, and the life cycle exergy by 33% (technical boundary) and 24% (physical boundary). Rey and Zmeureanu[16] optimized an SWHS for a residential building using a PSO/HJ hybrid algorithm. The life cycle cost and life cycle energy were reduced by 11.4% and 36.1%, respectively. There is no general rule for optimization algorithm selection of SWHS because of both the complex structure and the variety of the intended use of those systems. However, it is possible to say that the authors usually benefit from GA, PSO, or hybrid algorithms. Some other important research studies are summarized as follows: Kalogirou[17] proposed an approach to design and optimization of various SWHSs with an artificial neural network and GA. The optimum collector area and storage tank volume were obtained in order to produce the maximum life cycle savings. Yaman and Arslan[18] suggested the optimization method in order to optimize life cycle cost for an SWHS. The obtained results showed that SF increased with an average of 35.4% and LCC decreased with an average of 4.5% in different climatic regions. Yan *et al.*[19] proposed an optimization method of providing the maximal life cycle energy saving. Recently, Araya *et al.*[20] and Karaçavuş[21] proposed SWHS optimization methodology that focused on cost efficiency, implemented for different climatic regions.

There are limited studies on the optimization of an SWHS for monthly or seasonal periods rather than the annual period. For example, Fahmy *et al.*[22] determined the optimum surface area of the flat plate collector of an SWHS to obtain the highest solar fraction on a monthly basis, and Li *et al.*[23] suggested that the storage tank volume corresponding to one unit collector area was between 0.01 and 0.02 m^3/m^2 in their work on storage volume and storage tank temperature. A similar study showed that using the multiple tank system is more efficient than the single tank with thermal stratification, according to the design method of SWHS that was proposed in the cold climate regions by Mori and Kawamura.[24] Their results showed that 20% of total hot water demand was provided by solar energy in the winter period for a cold region, whereas sufficient thermal performance could be obtained in the summer period. Hobbi and Siddiqui[25] stated that the designed SWHS according to the optimum parameter values of the solar collector surface area and mass flow rate, fluid type, storage tank volume and height, heat exchanger effectiveness, size and length of connecting pipes, and type of absorber plate material could provide for 83%–97% and 30%–68% of the hot water demands in summer and winter.[25] Hasan[26] performed a parametric study on the optimum collector angle of inclination and tank volume and position on a monthly basis for a thermosyphon solar water heater. System performance increased by 5% using a smaller storage tank placed 0.5 m above the collector bottom header at the optimum collector angle of inclination.[26] However, only design solutions based on the annual basis were discussed in detail. In addition, many researchers have investigated the optimum orientation of the collector and/or the angle of the solar collector inclination for monthly, seasonal, and annual periods.[27–30]

The survey of the literature showed that the optimization of the SWHS components (e.g., storage tank, solar collector, and auxiliary water heater) has been carried out according to thermal, economical, and/or environmental aspects in annual or long-term periods. The optimum design results obtained over short time periods are required for extreme cold/hot climatic conditions or special applications, such as a greenhouse rather than annual or long-term periods. Using this approach, the thermal and economic performance of the system would be increased. On the other hand, whereas many researchers perform design and optimization of SWHS with cost efficiency such as life cycle cost,[11,13] life cycle savings,[20] and payback period,[31] they could ignore certain contribution of solar energy, which is crucial for sustainability. When the studies are evaluated in this direction, the obtained results can be very different.

In this study, optimum SWHS design parameters (storage tank volume and number of solar collectors) are determined for five different climatic regions of Turkey. The optimization procedure including the LCC analysis constraint to 40% SF was carried out for annual and seasonal periods. PSO[32] and the HJ[33] hybrid optimization algorithm (PSO/HJ) were used in the procedure. Finally, the parametric sensitivity analysis was performed to investigate the effect of water temperature demand, daily total amount of hot water required, and domestic hot water (DHW) profiles on an optimum SWHS design. The remainder of this paper is organized as follows: First, the simulation model is described and the optimization problem is defined in Sec. II. Then, the hybrid optimization algorithm (PSO/HJ) is explained in detail in Sec. III. In Sec. IV, the SWHS simulation and sensitivity analysis results are presented and discussed.

II. SYSTEM SIMULATION AND DESCRIPTION

A conventional SWHS was designed for a single-family house. The basic components of the system are given in Fig. 1. There is a closed loop system composed of a flat plate solar collector, a hot water storage tank assisted with a natural gas fired heater, a circulation pump, piping, and controls. The energy simulation of the SWHS was undertaken using EnergyPlus© (v8.4), a widespread and accepted tool in the global energy analysis community.[34] Among the other popular simulation tools such as BLAST (Building Loads Analysis and System Thermodynamics), BSim (Building Simulation), DeST (Designer's Simulation Toolkit), eQuest (Quick Energy Simulation Tool), and TRNSYS (TRaNsient SYtem Simulation), EnergyPlus is defined as completely implemented for modeling characteristics such as simulation solution, time step approach, simultaneous radiation and convection, solar gains, shading, and sky considerations.[35] The simulation model is described in the subsections II A–II E.

A. Reference climatic conditions

To evaluate the effect of the climate on the performance of the SWHS, five major climatic regions of Turkey were considered according to the TS825 standard,[36] Ankara (mild-dry), Erzincan (cold), Erzurum (severe cold), Istanbul (mild-humid), and Mersin (warm). One-year EnergyPlus simulations were carried out with a typical meteorological year (TMY) weather file (time resolution 1 h) generated using Meteonorm© software. The climatic conditions are summarized in Table I.

B. Flat plate solar collectors

The solar collector was selected from the product list of ACR Solar Company.[37] The net surface area of the solar collector was 0.93 m^2, and four collectors were installed in the system.

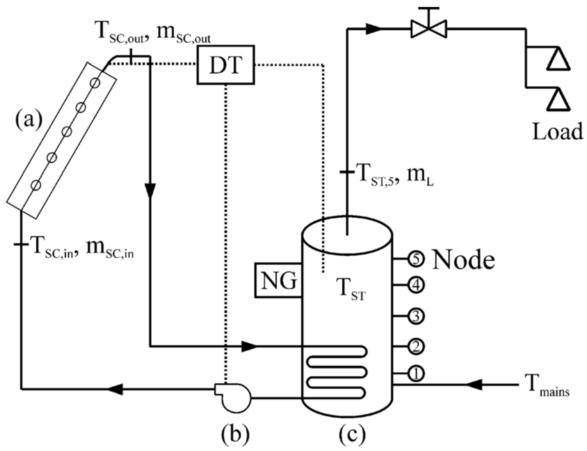

FIG. 1. The solar water heating system: (a) Flat plate collector; (b) pump; (c) storage tank assisted with a natural gas heater; NG: Natural gas; and DT: Differential thermostat.

The orientation of the face of the solar collector was in the southerly direction with a slope angle of the latitude of the region. The thermal efficiency of the collector was defined using the Hottel-Whillier-Bliss equation[38] given in the ASHRAE handbook

$$\eta = \frac{Q_{SC}}{I_{solar}A_{SC}} = F_R(\tau\alpha)_n - F_R U_L \frac{(T_{in,SC} - T_{amb})}{I_{solar}} + F_R U_{L2} \frac{(T_{in,SC} - T_{amb})^2}{I_{solar}}, \tag{1}$$

or

$$\eta = a_0 K_\theta - a_1 \frac{(T_{in,SC} - T_{amb})}{I_{solar}} + a_2 \frac{(T_{in,SC} - T_{amb})^2}{I_{solar}}, \tag{2}$$

where a_0 is the optical efficiency and a_1 and a_2 are the first order and second order heat loss coefficients, respectively. These coefficients were determined according to the Solar Rating & Certification Corporation (SRCC)[39] test results as $a_o = 0.6$, $a_1 = -3.87$, and $a_2 = 0.002$. T_{in} is the temperature of the water at the inlet of the solar collector, and T_{amb} is the ambient air temperature. Finally, I_{solar} is the solar radiation on the solar collector surface.

The actual thermal efficiency of a collector depends on the incidence angle of the solar radiation. The incidence angle modifier for the direct and diffuse component of the solar radiation is expressed as follows:

$$K_\theta = 1 - b_0 \left[\frac{1}{\cos(\theta)}\right] - b_1 \left[\frac{1}{\cos(\theta)}\right]^2, \tag{3}$$

where θ represents the incidence angle and b_o and b_1 are −0.194 and −0.019, respectively.

TABLE I. Key weather data for each region.

					Global solar radiation (kWh/m²)		Min/max temperature (°C)	
Regions	Climate	Latitude (°N)	Longitude (°E)	Altitude (m)	Summer	Winter	Summer	Winter
Ankara	Mild-dry	40.0	32.9	902	580.8	843.1	14.1/28.9	−9.9/23.8
Erzincan	Cold	39.7	39.5	1215	604.7	862.7	14.2/28.1	−15.3/20.8
Erzurum	Severe cold	40.0	41.3	1823	506.3	991.5	13.6/23.9	−25.9/15.5
Istanbul	Mild-humid	41.0	29.1	33	842.6	507.9	10.9/29.3	−1.4/18.9
Mersin	Warm	36.4	34.0	15	1411.7	285.7	12.6/33.8	3.5/17.1

C. Stratified storage tank

The volume of the storage tank was 200 l, and the height to diameter ratio was 3. The overall heat loss coefficient was assumed to be 0.8 W/m^{2}K. The temperature difference in the storage tank affects the SWHS thermal performance. Therefore, the stratification in the tank was taken into account in the calculation procedure. The cylindrical storage tank was divided into five nodes at an equal distance. The energy balance at each node defined by Araya *et al.*[20] and Duffie and Beckman[40] is given in Eqs. (4)–(8)

$$M_{ST,n}\frac{dT_{ST,n}}{dt} = U_{ST}A_{ST,n}(T_{amb} - T_{ST,n}) + \frac{kA_{ST,n+1}(T_{ST,n+1} - T_{ST,n})}{\Delta x} + \frac{kA_{ST,n-1}(T_{ST,n-1} - T_{ST,n})}{\Delta x} + \dot{Q}_{n+1} + \dot{Q}_{n-1} + \dot{Q}_1 + \dot{Q}_5 + \dot{Q}_{aux}, \tag{4}$$

where

$$\dot{Q}_{n+1} = (\dot{m}_L - \dot{m}_{SC})c_p(T_{ST,n+1} - T_{ST,n}), \quad \text{if } \dot{m}_{SC} < \dot{m}_L, \tag{5}$$

$$\dot{Q}_{n-1} = (\dot{m}_{SC} - \dot{m}_L)c_p(T_{ST,n-1} - T_{ST,n}), \quad \text{if } \dot{m}_{SC} > \dot{m}_L, \tag{6}$$

$$\dot{Q}_1 = \dot{m}_L c_p T_{mains} - \dot{m}_{SC} c_p T_{ST,1}, \quad \text{if } n = 1, \tag{7}$$

$$\dot{Q}_5 = \dot{m}_{SC} c_p T_{out} - \dot{m}_L c_p T_{ST,5}, \quad \text{if } n = 5, \tag{8}$$

where the storage tank inlet of water mains is located on node 1 and the outlet of the storage tank is located on node 5. M is the storage tank mass, m is the flow rate, T is the temperature, and A and U are the storage tank area and overall heat loss coefficient, respectively. *SC*, *L*, *ST*, *amb*, and *mains* subscripts represent the solar collector, load, storage tank, ambient, and mains water, respectively.

D. Load

When the solar energy was not sufficient to provide hot water demand, a natural gas operated heater was used in the storage tank. The auxiliary energy ($\dot{Q}_{aux}$) to heat the water in the storage tank to the set temperature with a natural gas fired water heater was calculated using the following equation:

$$\dot{Q}_{aux} = \eta_{aux}\dot{m}_L c_p(T_L - T_{ST,n=5}), \tag{9}$$

where η_{aux} is the thermal efficiency of the natural gas-fired water heater. Thus, the system load ($\dot{Q}_L$) is calculated using the following equation:

$$\dot{Q}_L = \dot{Q}_{SC} + \dot{Q}_{aux} - \dot{Q}_{loss}. \tag{10}$$

E. Control strategy

A variable speed pump was used to circulate the water between the solar collector and the storage tank. A differential thermostat was used to compare the temperature in the storage tank with the temperature in the solar collector outlet. If the temperature difference is higher than 5 °C, then the circulating pump starts and stops when that difference is below 2 °C. Thus, the pump is only turned on when there is a useful heat gain.

In the SWHS, the hot water usage instantaneous peak value was assumed to be 0.08 l/s and the total amount of hot water demand was 300 l at 55 °C. A time-dependent hot water usage profile was defined according to ASHRAE 90.2[41] standard.

III. OPTIMIZATION FRAMEWORK

In this study, the optimum design solutions of an SWHS were determined using a hybrid optimization algorithm, PSO/HJ. Wetter and Wright[42] stated that the combination of PSO and HJ algorithms improves the optimization performance, despite the hybrid algorithm having been chosen for a few studies[43] in the literature. PSO was proposed by Kennedy and Eberhart[44,45] and further developed by Clerc and Kennedy[32] with a constriction coefficient algorithm. PSO is a population-based optimization method inspired by the social behavior of birds and bird-like species. The particles (solution) in the population randomly generated by the PSO algorithm are assigned to their random initial positions (x) and velocities (v) using the following equations:

$$v_i^{k+1} = X\left[v_1^k + c_1\varphi_1^k\left(p_{l,i}^k - x_i^k\right) + c_2\varphi_2^k\left(p_{g,i}^k - x_i^k\right)\right], \tag{11}$$

$$x_i^{k+1} = x_i^k + v_i^{k+1}, \tag{12}$$

where i is the number of particles and k is the number of iterations. $p_{l,i}$ is the position of the lowest cost function for the ith particle and $p_{g,i}$ is the position of the best particle in all previous generations. φ_1 and φ_2 are the randomly generated numbers between 0 and 1. Acceleration constants are selected as $c_1 = c_2 = 2.05$.[32] The PSO performance is improved by controlling the particle velocity with the constriction factor X. The constriction factor is calculated using the following equation:[46]

$$X = \frac{2}{\left|2 - \omega - \sqrt{\omega^2 - 4\omega}\right|}, \tag{13}$$

where $\omega = c_1 + c_2 = 4.1$.

The particles change their velocity and position relative to the best solution in the population. In this way, generations are updated to obtain the most appropriate values. The solution of the PSO algorithm is chosen as the starting point for the HJ algorithm. The HJ pattern search algorithm is a direct search method proposed by Hooke and Jeeves.[33] HJ finds the local minimum for the most appropriate solution according to the neighborhood relation at each iteration. The successful values obtained by HJ are assigned as the optimum solutions. The control parameters of the PSO/HJ hybrid algorithm are listed in Table II.

The optimization problem of SWHS was solved using GenOpt® (v3.1), an optimization program for the minimization of a cost function evaluated by EnergyPlus. In Fig. 2, a general flow chart diagram of the SWHS optimization procedure is presented. EnergyPlus needs an input file that describes the SWHS and the environment surrounding it. After the simulation has

TABLE II. Settings of the SPO/HJ algorithm used for the optimization.

Parameter[a]	Value
Neighborhood topology	Von Neumann
Number of particles/generations	10/10
Cognitive/social acceleration	2.05/2.05
Maximum velocity gain continuous/discrete	0.5/4
Constriction gain	0.7298
Mesh size divider	2
Initial mesh size exponent	0
Mesh size exponent increment	1
Number of step reductions	4

[a]The first five rows for PSO and the last four parameters for HJ algorithms are user-defined.

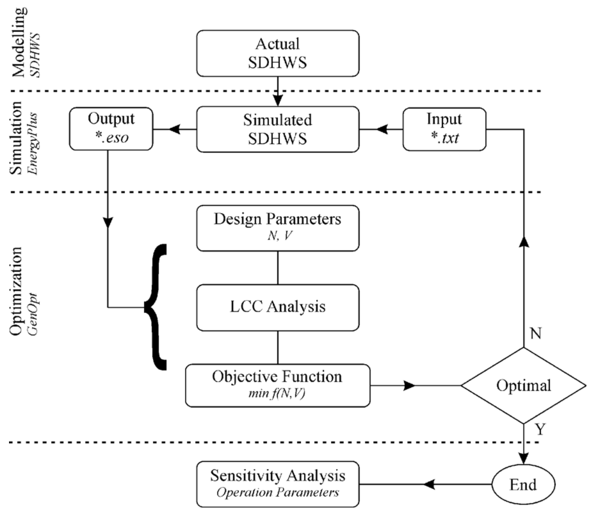

FIG. 2. The optimization procedure.

been completed, the required output data listed in the EnergyPlus raw report variable output file (*.eso) were transferred to the algorithm written in Java platform in the GenOpt program. The optimization algorithm examined the minimum value of the objective function by changing the values of the design parameters and calculating LCC. After the optimum solution was achieved, a sensitivity analysis was carried out to determine the effects of operating parameters.

A. Decision variables

In the optimization procedure of the SWHS, the solar collector number (N_{SC}) and storage tank volume (V_{ST}) were taken as independent parameters and decision variables in the optimization problem were obtained according to the vector of those parameters given in the following equation:

$$\vec{x} = [N_{SC},\, V_{ST}]^T, \tag{14}$$

$$\vec{x} \triangleq \left\{(N_{SC},\, V_{ST}) \in \mathbb{Z}^n \times \mathbb{R}^n | a^i \le x^i \le u^i; i \in (1, \ldots, n)\right\}, \tag{15}$$

where a^i and u^i denote the lower and upper limit, respectively. The optimization problem handled the discrete variables for $N_{SC} \in \{1,\, 2,\, \ldots,\, 12\}$ and continuous variables for $V_{ST} \in \{5, \ldots, 1000\}$.

B. Objective function

The objective function, also called the cost function, is what is optimized in optimization problems. The appropriate identification of this function is important to accurately solve the problem. In the optimization problem of SWHSs, some researchers[12,47] defined the cost function according to the SF, whereas some authors[11,13] defined this according to LCC. In this study, the cost function was considered as LCC with the constraint for SF. Therefore, the cost function was defined according to LCC, and SF was set as a constraint condition to ensure that the optimum solution was a practical design. The cost function was formulated as

$$\min : f(\vec{x}) \triangleq \sum_{i=1}^{n} LCC_i(\vec{x}) + \begin{cases} 0, \; SF(\vec{x}) \ge 0.4 \\ \infty, \; otherwise. \end{cases} \tag{16}$$

The LCC of an SWHS comprises three main components: investment cost C_{inv}, operation and maintenance cost $C_{O\ \&\ M}$, and energy cost C_E. LCC is given as

$$LCC = C_{inv} + (C_{O\,\&\,M} + C_E)PW, \tag{17}$$

where

$$C_{inv} = C_{SC}N_{SC} + C_{ST}V_{ST} + C_{pump}, \tag{18}$$

$$C_{O\,\&\,M} = \frac{C_{inv}}{t}0.10, \tag{19}$$

and

$$C_E = \frac{Q_{aux}C_{NG}}{\eta_{aux}} + \frac{Q_{pump}C_{elek}}{\eta_{pump}}, \tag{20}$$

where C_{SC}, C_{ST}, and C_{pump} represent the solar collector, storage tank, and pump costs, respectively, and t is the life-time. The electricity C_{elek} and natural gas C_{NG} costs were assumed to be 0.116 \$/kWh and 0.267 \$/m^3. In Table III, the related costs used in the determination of the objective function are given in US Dollars. The present worth factor (PW) is calculated using the following expression:

$$PW = \frac{1 - (1 + int^*)^{-t}}{int^*}, \tag{21}$$

$$i^* = \frac{int - e}{1 + e}, \tag{22}$$

where *int* is the interest rate (10% in Turkey), e is the inflation rate (9% in Turkey), and life-time is assumed as 25 years. Finally, the solar fraction is determined using the following equation:

$$SF = (Q_L - Q_{aux})/Q_L. \tag{23}$$

IV. RESULTS AND DISCUSSION

In this study, the basic components of an SWHS were optimally sized, considering the climate, energy, and cost criteria for both annual and seasonal periods. The results of the optimization procedure were in parallel for all regions. In order to present the obtained results more clearly, the final outcomes of the optimization procedure related to all regions were given. It was chosen to discuss the detailed optimization results from Mersin due to the long sunshine duration and high solar radiation that make an SWHS preferable. The results were presented under the headings of the validation of the simulation, optimization, effect of the design parameters on performance, and sensitivity analysis.

A. Validation of the simulation results

Prior to the optimization process, the reliability of the mathematical model of the SWHS used in this study was investigated. The validation of the model was undertaken by comparison

TABLE III. Related costs used in the LCC analysis.

Component	Value[a]	Unit	References
Solar collector	87.3	\$/m^2	48
Storage tank	0.87 V_{ST}+188.4	\$/m^3	48
Circulation pump	249.7	\$	48
Natural gas	0.267	\$/m^3	49
Electricity	0.116	\$/kWh	49

[a]The exchange rate was taken as 1 TL = 3.54 \$ in consideration of May 2, 2017.

with experimental studies in the literature. Ayompe and Duffy[50] investigated the thermal performance of an SWHS with flat plate collectors in Focas Institute, Dublin, Ireland (53.33° N, 6.25° W), and presented the experimental results of the daily, monthly, and annual performance. Similar operating conditions were introduced to the EnergyPlus© simulation file. Since the meteorological data obtained at the time of the experiments were not available, the TMY file that includes the long-term average data of Dublin was used. In Fig. 3(a), comparison of the monthly average auxiliary energy consumption rate of the SWHS obtained in simulations with experimental data is given. In Fig. 3(b), the same comparison was undertaken for the SF. The mean absolute percentage error (MAPE) and root mean square error (RMSE) were obtained to be 11.66% and 39.24 kWh, respectively, for the auxiliary energy consumption rate. For SF, MAPE and RMSE were calculated to be 15.91% and 6.92%, respectively. The main reason for the acceptable deviations was the use of the long-term average meteorological data especially solar radiation rather than the data measured during the experiments. Moreover, the other reasons for the deviations included the adiabatic pipe assumption and neglecting pressure losses.

B. Optimization results

The annual and seasonal optimization results of the SWHS for each region are presented in Fig. 4 as a Pareto front, and the obtained optimum technical parameters (storage tank volume and solar collector number) and the performance parameters (LCC and SF) are presented in Table IV. The optimization process showed that LCC could be reduced for all regions in the range of 3.3%–5.8% and 1.8%–4.8% in the annual and summer simulation period, respectively. The highest reduction in LCC was obtained for Mersin (warm region) by 5.8% in the annual simulation period [Fig. 4(e)] and for Erzurum (severely cold region) by 4.8% in the summer season period [Fig. 4(c)]. However, it was observed that in all regions except Ankara, the optimum LCC values increased from 1.1% to 4.6% in the winter simulation period. The main reason for this increase was the high solar collector number, providing a 40% SF constraint. In fact, the sunshine duration for SWHS is the most important effect and is for winter less than summer.[51] Moreover, heat losses from the system are higher in winter than in summer. Nevertheless, the cost function achieved the minimum of 40% energy savings in the winter season. In this regard, reducing fossil fuel consumption has led to a more sustainable system, despite the increase in LCC.

In Fig. 4, the clear effect of the proposed optimization method on the SF was observed. The optimization process showed that SF increased for all regions in the range of 31.4%–44.9% and 15.2%–64.1% in the annual and winter simulation period, respectively. In the summer season, SF only increased in Mersin by 10.7%, whereas a 6.5% to 16.1% decrease was observed among all regions. In addition, the optimum solutions provided the minimum of 40% contribution of solar energy during all simulation periods. The optimum solutions obtained without any constraint on SF could sometimes lead to inadequate solar energy contribution in

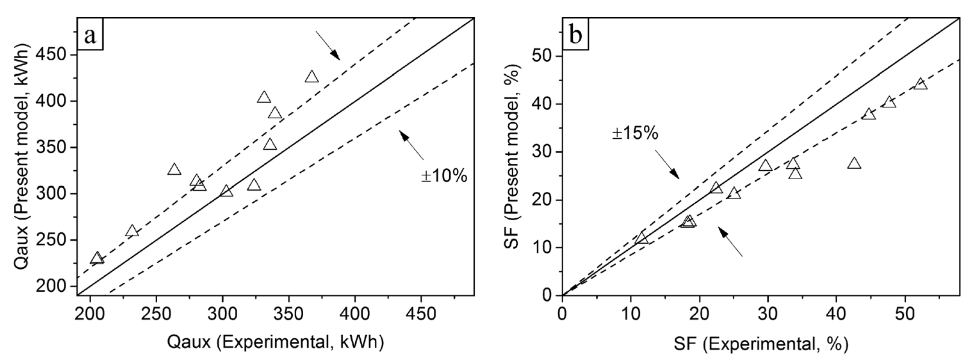

FIG. 3. Comparison of simulation results in the current study with the results found by Ayompe and Duffy:[50] (a) auxiliary energy consumption rate and (b) solar fraction.

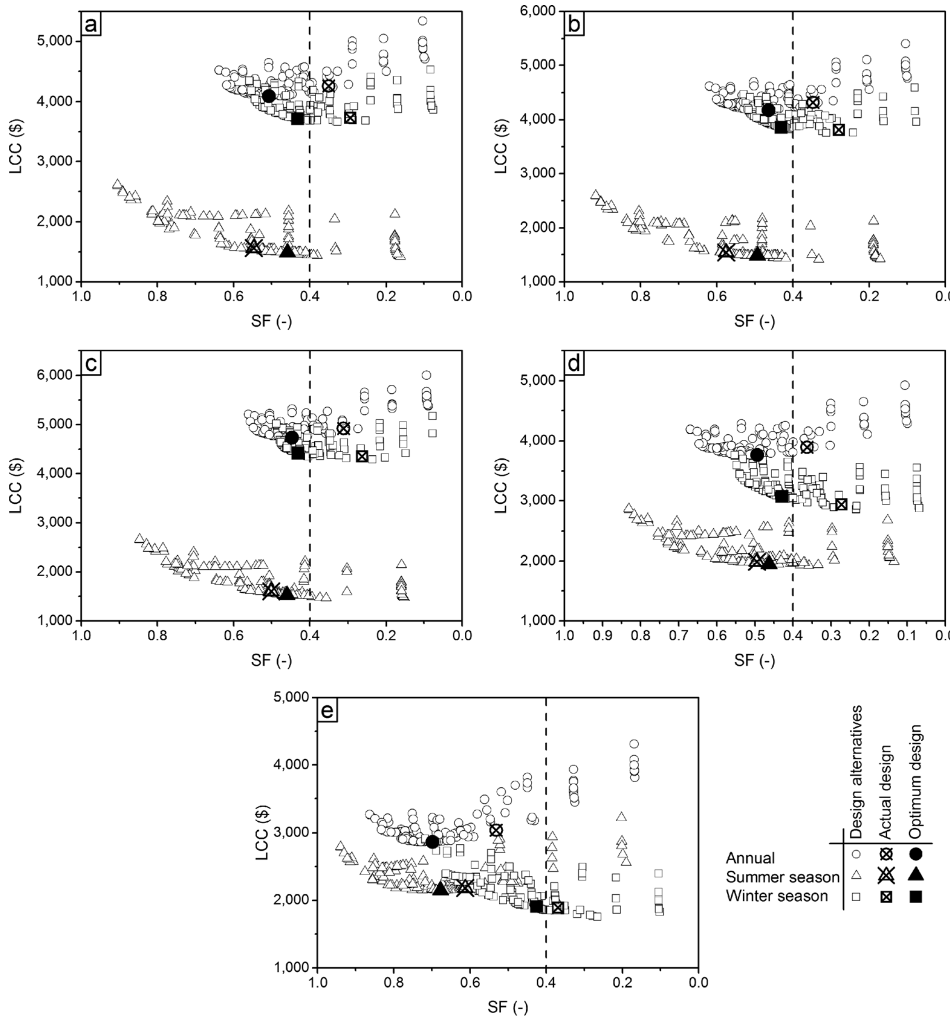

FIG. 4. Pareto front of the annual and seasonal optimization results (SF vs. LCC) in (a) Ankara; (b) Erzincan; (c) Erzurum; (d) Istanbul; and (e) Mersin.

the winter period or vice versa in the summer period.[24,25] The contribution of the solar energy cannot be ignored on SWHS with an auxiliary heater, especially for the winter period or cold regions. A linear relation was observed between LCC and SF for all regions (Fig. 4). Similar results were obtained when the relation between the storage tank volume and SF was examined. Since the optimum number of solar collectors did not show any significant difference between the regions, it was found that increasing SF led to an increase in the storage tank volume and a reduction in LCC. Thus, an increase in SF led to an increase in the investment cost, while the operation and energy costs were reduced. Bornatico *et al.*[14] obtained similar results, indicating that total cost could be reduced as well as an increase in SF. The economic and thermal performance of an SWHS can be improved by creating a design according to the certain climatic conditions.

In Figs. 5–7, the optimization results of the SWHS in Mersin are given for annual and seasonal simulation periods. In Fig. 5, the optimization procedure is shown for each iteration. The PSO/HJ optimization algorithm obtained the minimum value of the cost function (2863.9 $) defined in Eq. (16) for the first time in the 144th iteration and converged in 195 iterations. The optimum results of the SWHS obtained for annual period were seven solar collectors and a hot water storage tank volume of 316.5 l. When compared with the actual SWHS, LCC was reduced by 5.8% and SF was increased by 31.4%. In Figs. 6 and 7, the optimization results for

TABLE IV. Optimization of cost function terms.

	Annual			Summer season			Winter season		
Term	Init. value	Opt. value	Dev. (%)	Init. value	Opt. value	Dev. (%)	Init. value	Opt. value	Dev. (%)
Ankara									
LCC ($)	4261.1	4091.4	−4.0	1561.2	1490.7	−4.5	3731.7	3713.7	−0.5
SF (-)	0.35	0.51	44.9	0.55	0.46	−16.1	0.29	0.43	47.3
V (l)	200.0	269.1	34.5	200.0	50.5	−74.8	200.0	221.7	10.8
N (U)	4	8	100.0	4	4	0	4	8	100.0
V_{ST}/A_{SC} (m^3/m^2)		0.036			0.014			0.030	
Erzincan									
LCC ($)	4319.8	4176.0	−3.3	1541.9	1482.3	−3.9	3813.9	3855.9	1.1
SF (-)	0.35	0.46	33.6	0.57	0.49	−14.3	0.28	0.43	54.3
V (l)	200.0	232.6	16.3	200.0	64.4	−67.8	200.0	235.1	17.5
N (U)	4	7	75.0	4	4	0.0	4	9	125.0
V_{ST}/A_{SC} (m^3/m^2)		0.036			0.017			0.028	
Erzurum									
LCC ($)	4920.1	4733.0	−3.8	1605.3	1528.2	−4.8	4351.9	4413.1	1.4
SF (-)	0.31	0.45	43.7	0.50	0.46	−8.3	0.26	0.43	64.1
V (l)	200.0	232.6	16.3	200.0	81.9	−59.1	200.0	295.3	47.7
N (U)	4	8	100.0	4	4	0.0	4	10	150.0
V_{ST}/A_{SC} (m^3/m^2)		0.031			0.022			0.032	
Istanbul									
LCC ($)	3894.8	3761.0	−3.4	1989.0	1943.2	−2.3	2938.3	3073.7	4.6
SF (-)	0.36	0.49	36.2	0.49	0.46	−6.5	0.27	0.43	57.0
V (l)	200.0	245.1	22.6	200.0	107.6	−46.2	200.0	196.5	−1.8
N (U)	4	7	75.0	4	4	0.0	4	9	125.0
V_{ST}/A_{SC} (m^3/m^2)		0.038			0.029			0.023	
Mersin									
LCC ($)	3038.9	2863.9	−5.8	2181.2	2142.1	−1.8	1891.6	1903.5	0.6
SF (-)	0.53	0.70	31.4	0.61	0.68	10.7	0.37	0.43	15.2
V (l)	200.0	316.5	58.3	200.0	217.0	8.5	200.0	178.6	−10.7
N (U)	4	7	75.0	4	5	25.0	4	5	25.0
V_{ST}/A_{SC} (m^3/m^2)		0.049			0.047			0.038	

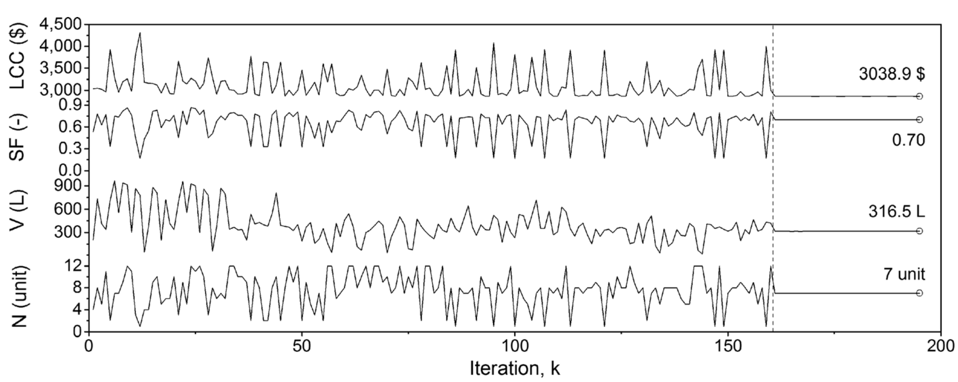

FIG. 5. Optimization of an actual SWHS for an annual period in Mersin; circle-marking: optimum solution and dashed-line: PSO ending-HJ beginning.

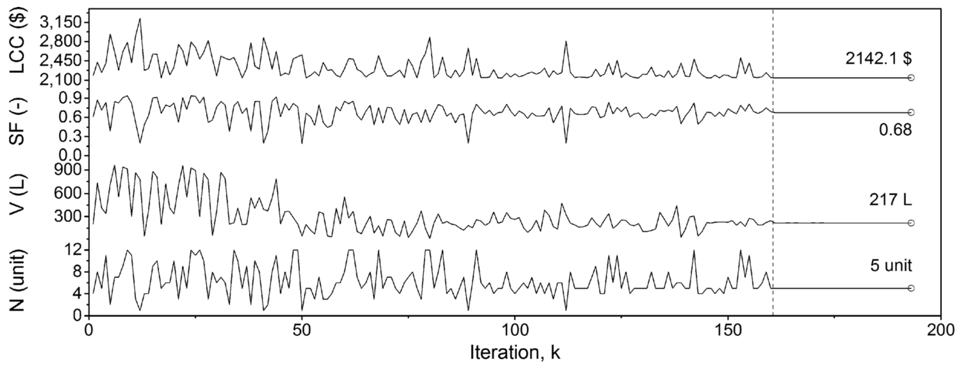

FIG. 6. Optimization of an actual SWHS for a summer season in Mersin; circle-marking: optimum solution and dashed-line: PSO ending-HJ beginning.

the summer and winter seasons are shown. The optimum results of the SWHS obtained for the summer season were five solar collectors and a storage tank volume of 217.0 l. For the winter season, a storage tank volume of 178.6 l was obtained with the same number of solar collectors obtained in the summer season. With the optimum SWHS, a saving of 1.8% for LCC in the summer season was achieved. However, LCC increased 0.6% in the winter season. Besides, a 10.7% and 15.2% increase in SF was obtained for the summer and winter seasons, respectively. For both annual and summer seasons, the results of the optimization processes showed that the increase in SF led to a decrease in the LCC of the SWHS with an increase in the storage tank volume. However, a decrease in the volume was obtained in the winter season optimization process. In general, the annual and summer season optimization processes showed similar characteristic behavior for the optimization of the SWHS parameters. However, the winter season optimization results revealed that they made a difference in terms of the relations between the parameters. This shows that the performance of an SWHS can be improved by creating a design that takes into account the seasonal conditions.

C. The effect of the design parameters on performance

In Fig. 8, the relation between LCC and the storage tank volume per unit collector area is presented. Only the solutions that met the SF > 0.4 conditions are shown. The others were eliminated since a solution with SF < 0.4 is an undesirable situation in the proposed study. Each solution created a design alternative that provides a range of certain contribution of solar energy. It is understood that there is a certain optimum volume-area ratio to achieve cost efficiency. Since the insufficient tank volume or the collector surface area leads to an increase in the energy cost, excess amount of those components leads to an increase in the investment cost.

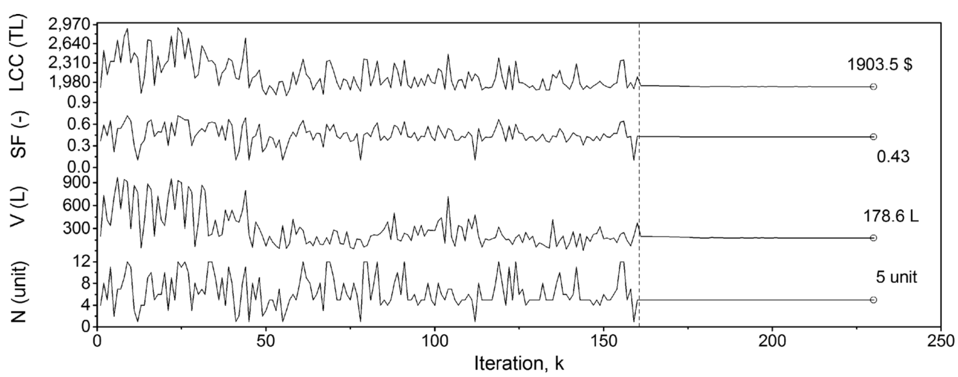

FIG. 7. Optimization of an actual SWHS for a winter season in Mersin; circle-marking: Optimum solution and dashed-line: PSO ending-HJ beginning.

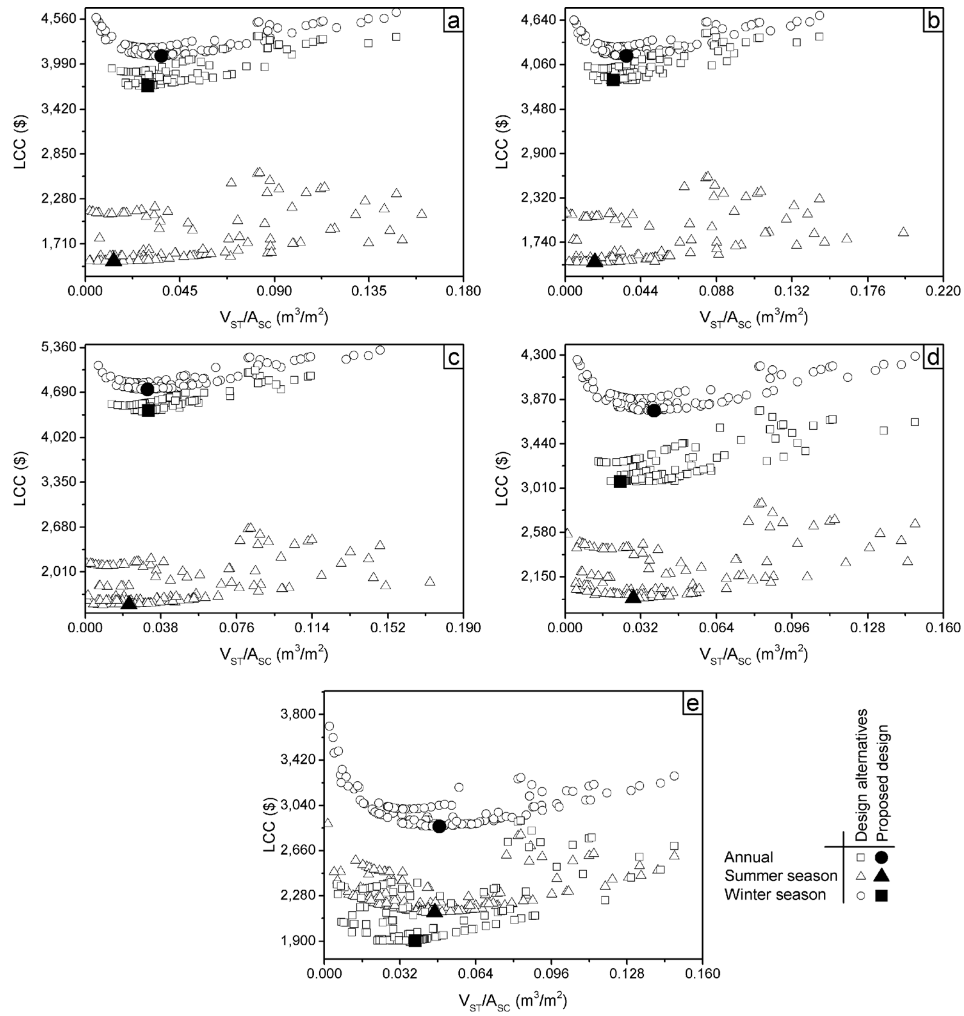

FIG. 8. The relation between LCC and the storage tank volume per unit collector area, (a) Ankara; (b) Erzincan; (c) Erzurum; (d) Istanbul; and (e) Mersin.

In Table IV, the optimum values of the volume-area ratio for each climatic region are given. In the annual simulation period, the optimum volume-area ratio ranged from 0.031 m^3/m^2 (Erzurum, severely cold region) to 0.049 m^3/m^2 (Mersin, warm region). Moreover, in a cold climatic region, the collector surface area increases, while the storage tank volume shrinks; correspondingly, the highest LCC values were obtained. The main reason for that is the system load being higher in the cold climatic regions than the warm climatic regions. Çomaklı *et al.*[52] investigated the volume-area ratio of SWHS in Erzurum, Turkey, experimentally. Their results showed that the volume-area ratio can be 0.05–0.07 m^3/m^2, where the collector efficiency was between 35% and 45%. However, the auxiliary heater was not used in the system and the effect of cost on the system was not examined. Thus, unnecessarily increasing both the storage tank volume and the collector area increases the investment cost. Besides that, decreasing the storage tank volume may lead to a decrease in thermal energy storage capacity of the system, which means high energy cost due to the auxiliary energy consumption. Using an insufficient number of solar collectors in the system also gives the same result. The proposed optimization method helps to clearly understand the behavior of the SWHS for designers on LCC and volume-area ratio.

On the other hand, the optimum volume-area ratio determined was in the range of 0.014–0.047 m^3/m^2 and 0.023–0.038 m^3/m^2 in the summer and winter season periods, respectively (Fig. 8). In both the summer and winter simulation periods, the highest optimum values of the volume-area ratio were obtained from Mersin. This situation, which is in line with the annual optimization results, was not observed for the smallest optimum volume-area ratio, which was obtained in Ankara (mild-dry climatic region) for the summer season and in Istanbul (mild-humid climatic region) for the winter season. The volume-area ratio results were close to each other in the annual and winter season analyses in the cold climatic region, while they were similar in the warm climatic region in the annual and summer season analyses. The results indicate that the design of an optimum SWHS according to the summer season conditions led to material saving and the design according to the winter season conditions increased the thermal performance of the system.

D. Sensitivity analysis results

A sensitivity analysis can be used to determine parameters that have a relative influence on the performance of a system. In this study, the relative influence of possible operating parameters on an optimum SWHS was investigated using a sensitivity analysis. The following three different operating parameters were selected: (i) temperature of the demanded domestic hot water (40 to 60 °C with 5 °C steps), (ii) total amount of daily DHW demand (150, 200, 300, 400, and 500 l/day), and iii) DHW profiles of ASHRAE 90.2,[41] Bouchelle *et al.*,[53] and SRCC[39] as given in Fig. 9. The sensitivity index[54] given in the following equation was used in the sensitivity analysis:

$$\delta f = (f_{max} - f_{min})/f_{max}. \tag{24}$$

The relative influence of the temperature of DHW, the total amount of daily DHW demand, and the DHW profiles on the optimized SWHS was examined for LCC and SF. The statistical results of the sensitivity analysis (max., min., avg., std. dev., and med.) for annual and seasonal periods for each location are given in Fig. 10. The optimized values of the variables are given in Table IV. The sensitivity analysis showed that LCC was most influenced by the daily total amount of DHW and SF was most influenced by DHW temperature for all regions. The DHW profile had the lowest influence on LCC and SF. The sensitivity analysis results obtained at different time periods did not make a difference to the order of the relative influence of the operating parameters on an optimum SWHS.

In Fig. 11, the relative influence of DHW temperature, the daily total amount of DHW, and the DHW profiles on LCC and SF of the optimum SWHS are given for Mersin. In the optimum SWHS determined according to the annual and seasonal periods, LCC was most influenced by the daily total amount of DHW [Fig. 11(b)] with a standard deviation of 0.09 for annual, 0.1 for the summer season, and 0.07 for the winter season. SF was most influenced by DHW temperature [Fig. 11(a)] with a standard deviation of 0.09 for annual, 0.13 for the summer season, and 0.18 for the winter season. The DHW profile had the lowest influence on LCC and SF with a standard deviation of 0.01 for both annual and seasonal periods.

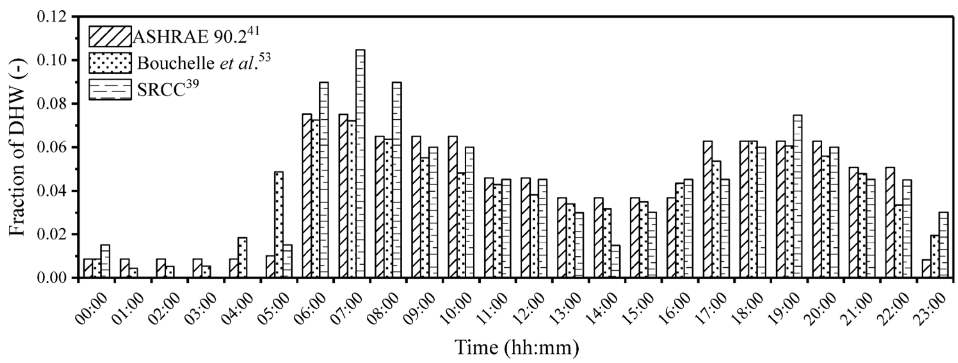

FIG. 9. DHW profiles.

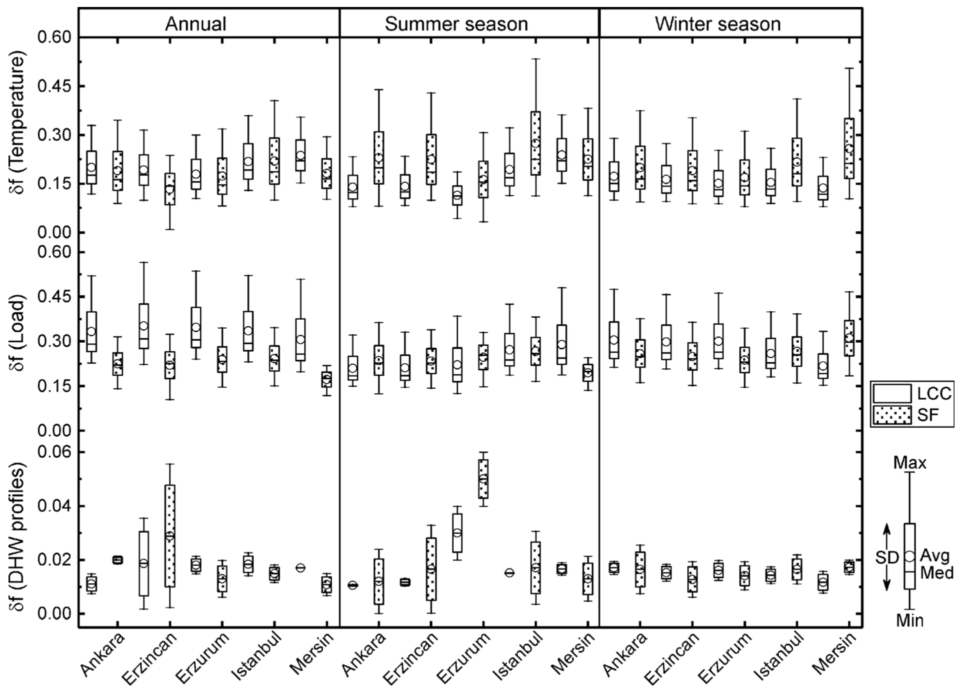

FIG. 10. Statistical results of the sensitivity analysis for annual and seasonal bases.

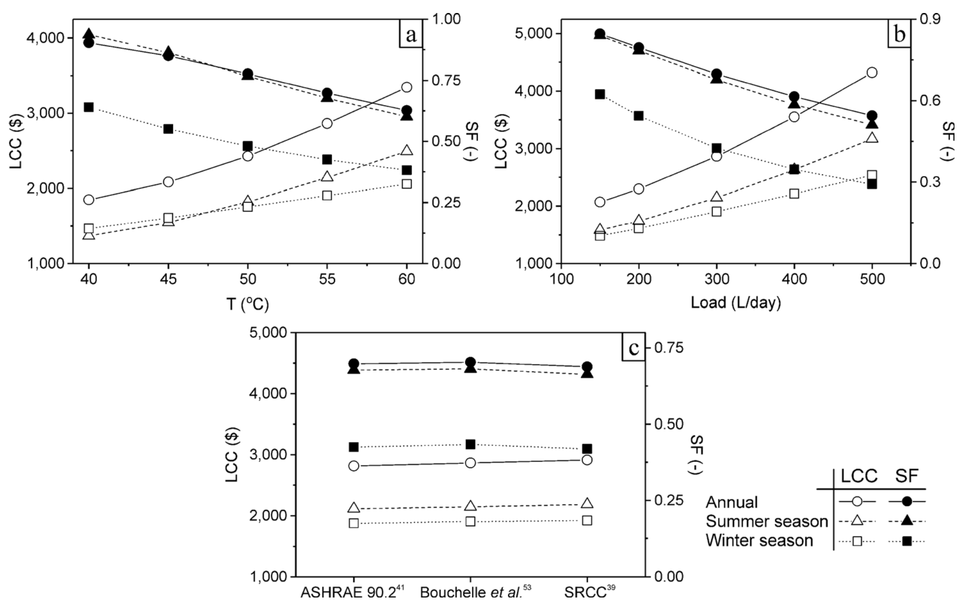

FIG. 11. The relative influence of different operating parameters on LCC and SF of the optimum SWHS in Mersin; (a) DHW temperature; (b) daily total amount of DHW; (c) DHW profiles.

V. CONCLUSIONS

In this study, the optimization of an SWHS was carried out according to the LCC criteria constrained with SF. The optimization procedure was conducted in different climatic regions for annual and seasonal simulation periods. The optimum technical parameters (storage tank volume and solar collector number) and the performance parameters (LCC and SF) of the SWHS were determined to meet the required load. The results obtained in this study are as follows:

(1) The optimum solution obtained in the annual simulation period showed that LCC was reduced by 3.3%–5.8% and SF was increased from 31.4% to 44.9%.Reduction in LCC was also achieved in the optimization process in the summer simulation period. However, in the winter simulation period, the same trend was not obtained for any of the regions except Ankara. SF increased for all regions in the range of 15.2%–64.1% in the winter simulation period. In the summer season, SF only increased in Mersin by 10.7%, whereas a 6.5%–16.1% decrease was observed among all other regions. All the optimum solutions ensure to achieve a minimum of 40% contribution of solar energy. Thus, the proposed optimum SWHS guarantees the minimum of 40% energy savings as well as cost efficiency during the optimization period. In this way, the economic and thermal performance can be stabilized in the systems designed by this proposed method in annual or season periods.
(2) The recommended values of the storage tank volume per unit collector area were between 0.031 and 0.049, 0.014 and 0.038, and 0.023 and 0.038 m^3/m^2 in the annual, summer, and winter simulation periods, respectively. It is possible to provide enough contribution of solar energy in annual or seasonal periods according to the recommended ratios. The optimum solutions focused on providing material savings in the summer season and increasing thermal performance in the winter season. To improve the performance of an SWHS, it is necessary to design the system according to the intended use and climatic conditions.
(3) A sensitivity analysis was carried out for three different operating parameters. LCC was the most affected by the daily total amount of DHW, whereas SF was the most affected by the DHW temperature. The DHW profile had the lowest effect on LCC and SF.

As a result, an appropriate design of an SWHS should be created according to the intended use of the systems, as well as energy, cost, and climate. In the design and optimization of the SWHS, it should be considered to provide certain energy savings related to different system capacities and market volumes in relation to the water heater fuel type that provides the specified load. In this way, these systems will be more sustainable. It is expected that the obtained results will be of interest to researchers, manufacturers, and technical experts. In future studies, more decision variables can be used, multi-objective optimization studies can be performed based on life cycle assessment, and the validity of the optimized value can be increased by calculating the system uncertainties.

NOMENCLATURE

A	Area, m^2
a_0, a_1, a_2	Efficiency equation coefficients
b_0, b_1	Incidence angle modifier coefficients
C	Cost, $
c_1, c_1	Acceleration constants, dimensionless
e	Inflation, %
F_R	Heat removal factor, dimensionless
I_{solar}	Solar radiation on the solar collector surface, W/m^2
int	Interest rate, %
K_θ	Incidence angle modifier, dimensionless
m	Mass flow rate, kg/s
M	Storage tank mass, kg
N	Number of solar collectors, u
Q	Heat transfer rate, W
SF	Solar fraction, dimensionless
t	Lifetime, yr
T	Temperature, °C
U	Overall heat loss coefficient, W/m^2 K
U_L	Solar collector transmittance, W/m^2 K

U_{L2}	Solar collector transmittance, W/m^2 K
v	Particle velocity
V	Volume, l
x	Particle initial position
$\vec{x}$	Vector of decision variables
X	Constriction factor, dimensionless

Greek symbols

δf	Sensitivity index
η_{aux}	Efficiency of the natural gas-fired water heater, 90%
η_{pump}	Pump efficiency, 90%
θ	Solar incidence angle, $^\circ$
$(\tau\alpha)_n$	Transmittance-absorptance at the normal incidence angle, dimensionless
φ_1, φ_2	Randomly generated numbers between 0 and 1

Subscripts and superscripts

amb	Ambient
aux	Auxiliary energy
E	Energy
elek	Electric
i	Number of particles
in	Inlet
inv	Investment
k	Iterations
L	Load
n	Node
O & M	Operation and maintenance
SC	Solar collector
ST	Storage tank

Abbreviations

Avg	Average
BLAST	Building load analysis and system thermodynamics
BSim	Building simulation
DeST	Designer's simulation toolkit
DHW	Domestic hot water
DT	Differential thermostat
eQuest	Quick energy simulation tool
GA	Genetic algorithm
HJ	Hooke and Jeeves algorithm
LCC	Life cycle cost
MAPE	Mean absolute percentage error
med	Median
NG	Natural gas
PSO	Particle swarm optimization algorithm
PW	Present worth
RMSE	Root mean square error
SD	Standard deviation
SWHS	Solar water heating system
TMY	Typical meteorological year
TRNSYS	Transient system simulation

[1]See http://ec.europa.eu/eurostat/web/energy/data for Eurostat data.
[2]H. C. Hottel and A. Whillier, in *Transactions of the Conference on the Use of Solar Energy* (University of Arizona Press, Tucson, AZ, USA, 1958), pp. 74–104.
[3]S. A. Klein, Sol. Energy **21**, 393 (1978).
[4]S. A. Klein, W. A. Beckman, and J. A. Duffie, Sol. Energy **18**, 113 (1976).
[5]S. A. Klein and W. A. Beckman, Sol. Energy **22**, 269 (1979).
[6]S. Colle and H. Vidal, Sol. Energy **76**, 125 (2004).
[7]See https://energyplus.net/ for EnergyPlus simulation tools, US DOE.
[8]See http://sel.me.wisc.edu/trnsys for TRaNsient SYstem Simulation Program (TRNSYS), University of Wisconsin Madison, USA.
[9]Watsun Simulation Laboratory, *User's Manual and Program Documentation* (Department of Systems Design Engineering, University of Waterloo, 1992).
[10]A. Al-Alili, Y. Hwang, R. Radermacher, and I. Kubo, Sol. Energy **84**, 2034 (2010).
[11]M. J. Ko, Energies **8**, 11380 (2015).
[12]J. Skerlić, J. Radulović, D. Nikolić, and M. Bojić, J. Renewable Sustainable Energy **5**, 041820 (2013).
[13]D. M. Atia, F. H. Fahmy, N. M. Ahmed, and H. T. Dorrah, Math. Comput. Model. **55**, 1436 (2012).
[14]R. Bornatico, M. Pfeiffer, A. Witzig, and L. Guzzella, Energy **41**, 31 (2012).
[15]J. Ng Cheng Hin and R. Zmeureanu, Sol. Energy **100**, 102 (2014).
[16]A. Rey and R. Zmeureanu, Sol. Energy **139**, 622 (2016).
[17]S. A. Kalogirou, Appl. Energy **77**, 383 (2004).
[18]K. Yaman and G. Arslan, Int. J. Eng. Res. Dev. **9**, 73 (2017).
[19]C. Yan, S. Wang, Z. Ma, and W. Shi, Renewable Energy **74**, 271 (2015).
[20]R. Araya, F. Bustos, J. Contreras, and A. Fuentes, Renewable Energy **112**, 365 (2017).
[21]B. Karaçavuş, J. Fac. Eng. Archit. Gazi Univ. **32**, 843 (2017).
[22]F. H. Fahmy, D. M. Atia, N. M. A. El-Rahman, and H. T. Dorrah, in *International Conference on Chemistry and Chemical Engineering* (IEEE, Kyoto, 2010), pp. 221–226.
[23]T. Li, Y. Liu, D. Wang, K. Shang, and J. Liu, Procedia Eng. **121**, 1356 (2015).
[24]T. Mori and A. Kawamura, Energy Procedia **48**, 1393 (2014).
[25]A. Hobbi and K. Siddiqui, Sol. Energy **83**, 700 (2009).
[26]A. Hasan, Int. J. Sol. Energy **17**, 135 (1995).
[27]M. Benghanem, Appl. Energy **88**, 1427 (2011).
[28]O. C. Aja, H. H. Al-Kayiem, and Z. A. A. Karim, J. Renewable Sustainable Energy **5**, 063112 (2013).
[29]E. A. Handoyo, D. Ichsani, and Prabowo, Energy Procedia **32**, 166 (2013).
[30]A. Z. Hafez, A. Soliman, and I. M. Ismail, Renewable Sustainable Energy Rev. **77**, 147 (2017).
[31]Y.-D. Kim, K. Thu, H. K. Bhatia, C. S. Bhatia, and K. C. Ng, Sol. Energy **86**, 1378 (2012).
[32]M. Clerc and J. Kennedy, IEEE Trans. Evol. Comput. **6**, 58 (2002).
[33]R. Hooke and T. A. Jeeves, J. ACM **8**, 212 (1961).
[34]M. Stadler, R. Firestone, D. Curtil, and C. Marnay, "*On-site generation simulation with EnergyPlus for commercial buildings,*" in *ACEEE Summer Study on Energy Efficiency in Buildings* (2006), pp. 242–254.
[35]V. S. K. V. Harish and A. Kumar, Renewable Sustainable Energy Rev. **56**, 1272 (2016).
[36]TS825, *Thermal Insulation Requirements for Buildings* (Turkish Standards Institution, Ankara, 2013).
[37]See http://www.acrsolar.com/ for ACR Solar.
[38]ASHRAE, *Handbook of Fundamentals* (American Society of Heating, Refrigerating and Air-Conditioning Engineers, Atlanta, GA, 2001).
[39]See http://www.solar-rating.org/ for the Solar Rating and Certification Corporation.
[40]J. A. Duffie and W. A. Beckman, *Solar Engineering of Thermal Processes* (John Wiley & Sons Inc., 2006).
[41]ASHRAE Standard 90.2-2001, *Energy Efficient Design of Low-Rise Residential Buildings* (American Society of Heating, Refrigerating and Air-Conditioning Engineers, Atlanta, GA, 2001).
[42]M. Wetter and J. Wright, Build. Environ. **39**, 989 (2004).
[43]A.-T. Nguyen, S. Reiter, and P. Rigo, Appl. Energy **113**, 1043 (2014).
[44]J. Kennedy and R. C. Eberhart, in *Conference on Neural Networks* (IEEE, Perth, Australia, 1995), pp. 1942–1948.
[45]J. Kennedy and R. C. Eberhart, in *Conference on Systems, Man, and Cybernetics* (IEEE, Orlando, FL, USA, 1997), pp. 4104–4108.
[46]M. Clerc, in *Proceedings of the ICEC* (IEEE, Washington, DC, USA, 1999), pp. 1951–1957.
[47]L. R. Bernardo, Energies **6**, 953 (2013).
[48]See http://www.csb.gov.tr/gm/donersermaye/index.php?Sayfa=haberdetay&Id=21332 for Republic of Turkey Ministry of Environment and Urbanization.
[49]See http://www.emra.org.tr/en/home for Republic of Turkey Energy Market Regulatory.
[50]L. M. Ayompe and A. Duffy, Appl. Therm. Eng. **58**, 447 (2013).
[51]K. Yaman and G. Arslan, "The impact of hourly solar radiation model on building energy analysis in different climatic regions of Turkey," Build. Simul. (published online).
[52]K. Çomaklı, U. Çakır, M. Kaya, and K. Bakirci, Energy Convers. Manage. **63**, 112 (2012).
[53]M. P. Bouchelle, D. S. Parker, and M. Anello, in *Proceedings of the Symposium on Improving Building Systems in Hot Humid Climates* (Texas A&M University, Texas, TX, USA, 2000).
[54]D. M. Hamby, Environ. Monit. Assess. **32**, 135 (1994).